JOURNAL OF MATERIALS SCIENCE **35** (2000) 1145–1152

Finite element analysis of characteristics of residual strains in cross-sectional specimens of strained-layer materials

C. R. CHEN, S. X. LI
State Key Laboratory for Fatigue and Fracture of Materials, Institute of Metal Research, Chinese Academy of Sciences, Shenyang 110015, People's Republic of China
E-mail: chrch@imr.ac.cn

A procedure for modeling effects of surface stress relaxation in specimens processed from materials with residual strains was described at first, then the anisotropic finite element analysis was performed to study characteristics of strain relaxation in the cross-sectional specimens of strained-layer materials. By using the "element death" technique, the finite element model of the specimen was separated from the finite element model of the bulk material, and a free surface was created. As a result, effects of surface stress relaxation during processing specimens were conveniently modeled. The finite element results about strain relaxation in the cross-sectional specimens of Ge_xSi_{1-x}/Si superlattice were presented. Characteristics about the shear strain near the interface, the strain normal to the surface, and the strain normal to the interface were studied. © *2000 Kluwer Academic Publishers*

1. Introduction

Residual microstrains have a great influence on electronic, mechanical and other properties of materials, thus an accurate knowledge of residual microstrain distribution is essential for developing advanced materials. Convergent beam electron diffraction (CBED) can accurately measure local strains in thin specimens due to the high spatial resolution of this technique. CBED has been applied to measure local strains in many materials, such as metal matrix composites [1, 2], strained-layer superlattices [3–5], nickel based superalloys [6], deformed copper [7, 8], epitaxial systems [9, 10], etc. However, one common problem mentioned in these CBED studies is the effects of surface stress relaxation of CBED specimens. For study by CBED, thin specimen must be prepared. Because surface stress relaxation occurs during the thinning process of specimens, residual strains in the specimens are different from that in the bulk material. When deducing strains in the bulk material from the measured strains in the specimen, effects of surface stress relaxation in the specimen should be taken into account [11].

For treating the effects of surface stress relaxation in specimens, one way is to understand the major factors affecting the surface stress relaxation, and take measures to minimize the effects of surface stress relaxation. Another way is to simulate the surface stress relaxation, and set up the relationship of residual strains between the thin specimen and the bulk material. Some researchers have applied the theoretical elastic method to study the elastic relaxation at a misfit interfaces of specimens [3, 4, 10, 12–14]. However, theoretical elastic method can only be applied to very simple geometry cases, and isotropic assumption is usually needed. Any problem that can be analyzed by theoretical elastic method can be conveniently solved by finite element (FE) method, thus the surface stress relaxation of specimen can be modeled by FE method. Some factors, such as complicated geometry, anisotropy, etc., are difficult for theoretical elastic method to treat, but are not difficult for FE method. The FE method has been applied to analyze elastic relaxation in CBED specimens of nickel based superalloys [6] and $In_xGa_{1-x}As$/GaAs strained-layers [15].

The purpose of this paper is to obtain the basic characteristics of strain relaxation in the cross-sectional specimens of multilayer materials by using the FE method. Anisotropy is considered. The distribution of residual strains in the specimen and the average strains of the whole specimen thickness are studied.

2. Method

2.1. The general procedure

In this paper, the procedure for modeling effects of surface stress relaxation during processing specimens from the bulk materials with residual strains has two steps:

Step 1: Design a FE model that can represent the bulk material. Part of this FE model is the FE model of specimen, i.e., the specimen is assumed to be within the bulk material. The residual strains in the FE model of the bulk material are assumed to be known, or are solved by FE method according to the given constraint and load conditions.

Step 2: Separate the FE model of the specimen from the FE model of the bulk material. This can be realized by deactivating the elements which do not belong to the FE model of specimen. The "element death" effect is achieved by multiplying the stiffness of the selected elements by a severe reduction factor (such as 10^{-6}). An element's stress, strain, load, heat, etc., are all set to zero as soon as the element is killed. When the selected elements are killed, a free surface is created, and thus surface stress relaxation occurs. As a result, effects of surface stress relaxation can be conveniently modeled. The "element death" effect can be very conveniently realized by using ANSYS software package.

2.2. The FE models

Suppose we have a multilayer material of alternating material A and material B. The layer thickness is t_A for each layer of material A and t_B for each layer of material B. The lattice is assumed to be cubic or tetragonal. Each interface is assumed to be coherent. The x-axis is normal to each layer. The y and z directions are assumed to be infinite. A specimen of thickness t with surfaces at $z = +t/2$ is processed from such material. The x-z section of specimen is shown as Fig. 1. The FE model of the bulk material is shown in Fig. 2. The 8-node 3-dimensional anisotropic element is used. The y-dimension of specimen is assumed to be infinite, thus only one layer of elements are needed along the y-direction of the FE model. The z-dimension of the FE model of bulk material is assumed to be $t/2 + \delta$, here δ is an arbitrary value. All nodes at $z = t/2 + \delta$ are constrained. When elements outside the plane $z = t/2$ are killed, the plane $z = t/2$ will be free, as a result, the FE model in Fig. 2 will become the FE model for the specimen. Two steps are needed for modeling effects of surface stress relaxation in the specimen: step 1, constructing residual strains in the FE model of the bulk material; step 2, separating the FE model of specimen from the FE model of the bulk material.

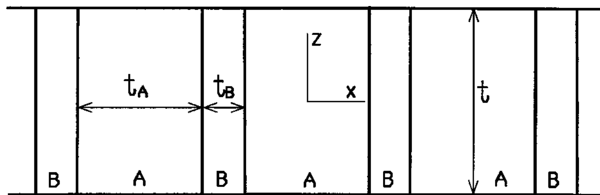

Figure 1 The x-z section of the specimen processed from the multilayer material ($z = +t/2$) are the specimen surfaces.

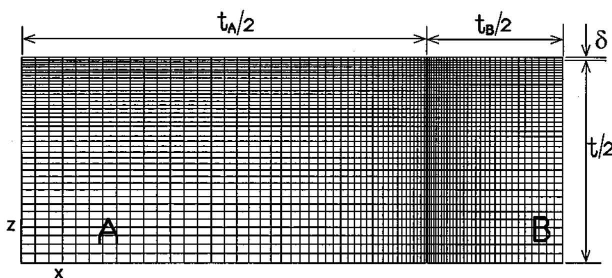

Figure 2 The FE models of specimen and the FE model of bulk multilayer material (this FE model is for the case: $t_A/t_B = 3$, $t/t_B = 3/2$).

2.2.1. Constructing residual strains in the FE model of the bulk material

Residual strains in the FE model of the bulk material can be assumed to be known or can be solved according to the given conditions of constraint and load. We assume residual strains in the bulk material are caused by the misfits of lattice constants between materials A and B. The misfits are: $f_a = (a_{02} - a_{01})/a_{01}$, $f_b = (b_{02} - b_{01})/b_{01}$, $f_c = (c_{02} - c_{01})/c_{01}$. Here, a_{01}, b_{01} and c_{01} are the lattice constants of material A; a_{02}, b_{02} and c_{02} are the lattice constants of material B. Residual strains in the FE model of the bulk material can be obtained by the fictitious thermal expansion. The fictitious thermal expansion coefficients are assumed to be $\alpha_a = \alpha_b = \alpha_c = 0$ for material A, and are assumed to be $\alpha_a = f_a$, $\alpha_b = f_b$ and $\alpha_c = f_c$ for material B. Here α_a, α_b and α_c are the fictitious thermal expansion coefficients along the orientations of [100], [010] and [001] respectively. Constraint, load, and material constants are as follows:

Constraint: $u_x = 0$ at $x = 0$; $u_y = 0$ at $y = 0$; $u_z = 0$ at $z = 0$; all nodes at $x = (t_A + t_B)/2$ have a common unknown u_x; all nodes at $y = d$ have a common unknown u_y (d: the y-direction thickness of the FE model); all nodes at $z = t/2 + \delta$ have a common unknown u_z.

Load: The temperature of the whole FE model changes $\Delta T = 1K$.

Material constants: For obtaining the basic characteristics of surface stress relaxation in cross-sectional specimens of the strained-layer materials, we use Ge_xSi_{1-x}/Si as an assumed material model. The Si and Ge_xSi_{1-x} have the same crystallographic orientations, and the lattices of both materials are cubic. We assume the orientations of Ge_xSi_{1-x}/Si to be $x(001)$, $y(1\bar{1}0)$, $z(110)$. Material constants are [16]:

$$\text{Si}: C_{11} = 165.8 \text{ GPa}, C_{12} = 63.9 \text{ GPa}, C_{44} = 79.6 \text{ GPa}, a_0 = 0.543 \text{ nm};$$

$$\text{Ge}: C_{11} = 124.0 \text{ GPa}, C_{12} = 41.3 \text{ GPa}, C_{44} = 68.3 \text{ GPa}, a_0 = 0.565 \text{ nm}.$$

Here C_{11}, C_{12} and C_{44} are elastic moduli, a_0 is the lattice constant. To keep a coherent interface between Si and Ge_xSi_{1-x}, we select $x = 0.1$. Let a_{01} and a_{02} represent the lattice constants of Si and Ge respectively, in the same way as in [4], the misfit between Si and Ge_xSi_{1-x} is defined as

$$f = x(a_{02} - a_{01})/a_{01} = 4 \times 10^{-3}$$

Because the content of Ge in Ge_xSi_{1-x} is low, moduli of Ge_xSi_{1-x} are similar to that of Si, for simplification, we assume the elastic constants C_{11}, C_{12} and C_{44} of Ge_xSi_{1-x} are the same as Si. For performing FE calculation, elastic modulus matrix of Si and

Ge_xSi_{1-x} under the coordinate system xyz is needed. In the same way as in [17], the elastic modulus matrix of Si and Ge_xSi_{1-x} under the coordinate system xyz is obtained as

$$[C] = \begin{bmatrix} 165.8 & & & & & \text{symmetry} \\ 63.9 & 194.45 & & & & \\ 63.9 & 35.25 & 194.45 & & & \\ 0 & 0 & 0 & 79.6 & & \\ 0 & 0 & 0 & 0 & 50.95 & \\ 0 & 0 & 0 & 0 & 0 & 79.6 \end{bmatrix}$$

2.2.2. Separating the FE model of specimen from the FE model of the bulk material

After residual strain fields in the FE model of the bulk material have been constructed (by assumption or by FE calculation), elastic relaxation of the thin specimen can be modeled by a very simple way: selected elements between $z = t/2$ and $z = t/2 + \delta$, then deactivate these elements by multiplying the stiffness of these elements by a reduction factor (10^{-6}). When these elements are deactivated, $z = t/2$ becomes a free surface, and elastic relaxation occurs. As a result, strains between $z = 0$ and $z = t/2$ become the residual strains in the specimen.

For understanding the effect of the thickness ratio of neighboring material layers, we select $t_A/t_B = 3$; for understanding the effect of the ratio of specimen thickness to the layer thickness, we select $t/t_B = 1/2$, $3/2$, $9/2$ and 8.

3. Results and discussion

Residual strains in the Ge_xSi_{1-x}/Si multilayer material have the characteristics: $\varepsilon_{yy} = \varepsilon_{zz}$, $\varepsilon_{xy} = \varepsilon_{yz} = \varepsilon_{xz} = 0$. Thus the lattice of each layer is strained as tetragonal structure. For $t_A/t_B = 3$, strains ε_{xx}, ε_{yy} and ε_{zz} in the bulk material are as follows:

$$\begin{aligned} \text{In } Ge_xSi_{1-x}\text{layer}: \varepsilon_{xx} &= 0.231\% \\ \varepsilon_{yy} = \varepsilon_{zz} &= -0.3\% \\ \text{In Si layer}: \varepsilon_{xx} &= -0.077\% \\ \varepsilon_{yy} = \varepsilon_{zz} &= 0.1\%. \end{aligned}$$

After surface stress relaxation, residual strain ε_{yy} in specimen is the same as in the bulk material; shear strains ε_{xy} and ε_{yz} are still zero. However, residual shear strain ε_{xz} is created at the interface; residual strain ε_{zz} is partly relaxed; residual strain ε_{xx} is also changed.

3.1. Distribution of residual strain ε_{xz} in specimens after surface stress relaxation

In the FE model of the bulk strained-layer material, there is no residual shear strain. When the FE model of specimen is separated from the FE model of the bulk material, compressive residual stress σ_{zz} of Ge_xSi_{1-x} and tensile residual stress σ_{zz} of Si are relaxed at the surface. Thus along the z direction, Ge_xSi_{1-x} extends, while Si contracts. However, Ge_xSi_{1-x} and Si must keep compatible at the interface, as a result, shear strain ε_{xz} is created at the interface.

Fig. 3 shows the distribution of residual strain ε_{xz} in specimens after surface stress relaxation. The ε_{xz} is zero at the center of each material layer, and is also zero at the thickness center of specimen. The maximal ε_{xz} is located at the local interface region a little below the surface. Along the interface, with the distance away from this local region, ε_{xz} decreases gradually. Near the surface, ε_{xz} decreases drastically with the distance away from the interface. The maximal ε_{xz} is affected by the ratio of specimen thickness to material layer thickness. The smaller this ratio is, the smaller the maximal ε_{xz} will be.

The ratios of specimen thickness to the layer thickness, i.e., t/t_A and t/t_B, have important effect on ε_{xz}. When both t/t_A and t/t_B are small (Fig. 3a), only a local region near the interface is distinctly affected by ε_{xz}; the distribution of ε_{xz} is nearly symmetrical about the interface. When $t/t_A = 1/2$ and $t/t_B = 3/2$ (Fig. 3b), the distribution of ε_{xz} near the interface is not symmetrical about the interface. When $t/t_A = 3/2$ and $t/t_B = 9/2$ (Fig. 3c), most part of the specimen is affected by ε_{xz}, and the region affected by ε_{xz} is wider in material A (Si) than that in material B (Ge_xSi_{1-x}). When both t/t_A and t/t_B are large (Fig. 3d), ε_{xz} has little effect at the region far from the surface.

3.2. Distribution of residual strain ε_{zz} in specimens after surface stress relaxation

Fig. 4 shows the distribution of residual strain ε_{zz} in specimens after surface stress relaxation. Residual strain ε_{zz} is larger at the interface, and decreases with the distance away from the interface. The local region at the intersection of interface and surface is a special region, where ε_{zz} decreases drastically with the distance away from the interface. The ratio of the specimen thickness to the layer thickness affects the characteristics of ε_{zz} distribution. When both t/t_A and t/t_B are small (Fig. 4a), in each material layer, ε_{zz} exists only near the interface, while ε_{zz} relaxes sufficiently throughout the specimen thickness at the region far away from the interface. When the specimen thickness is increased (Fig. 4b), the ε_{zz} region near the interface becomes wider. When both t/t_A and t/t_B are large (Fig. 4d), relaxation of ε_{zz} is distinct near the surface, while elastic relaxation has little effect on ε_{zz} at the region far away from the surface. From Fig. 4c and d we know the smallest ε_{zz} is not at the surface, but a little distance away from the surface.

3.3. Distribution of residual strain ε_{xx} in specimens after surface stress relaxation

Fig. 5 shows the distribution of residual strain ε_{xx} in specimens after surface stress relaxation. When both t/t_A and t/t_B are small (Fig. 5a), ε_{xx} decreases with the distance away from the interface; ε_{xx} near the surface is larger than that inside the specimen; at the region far

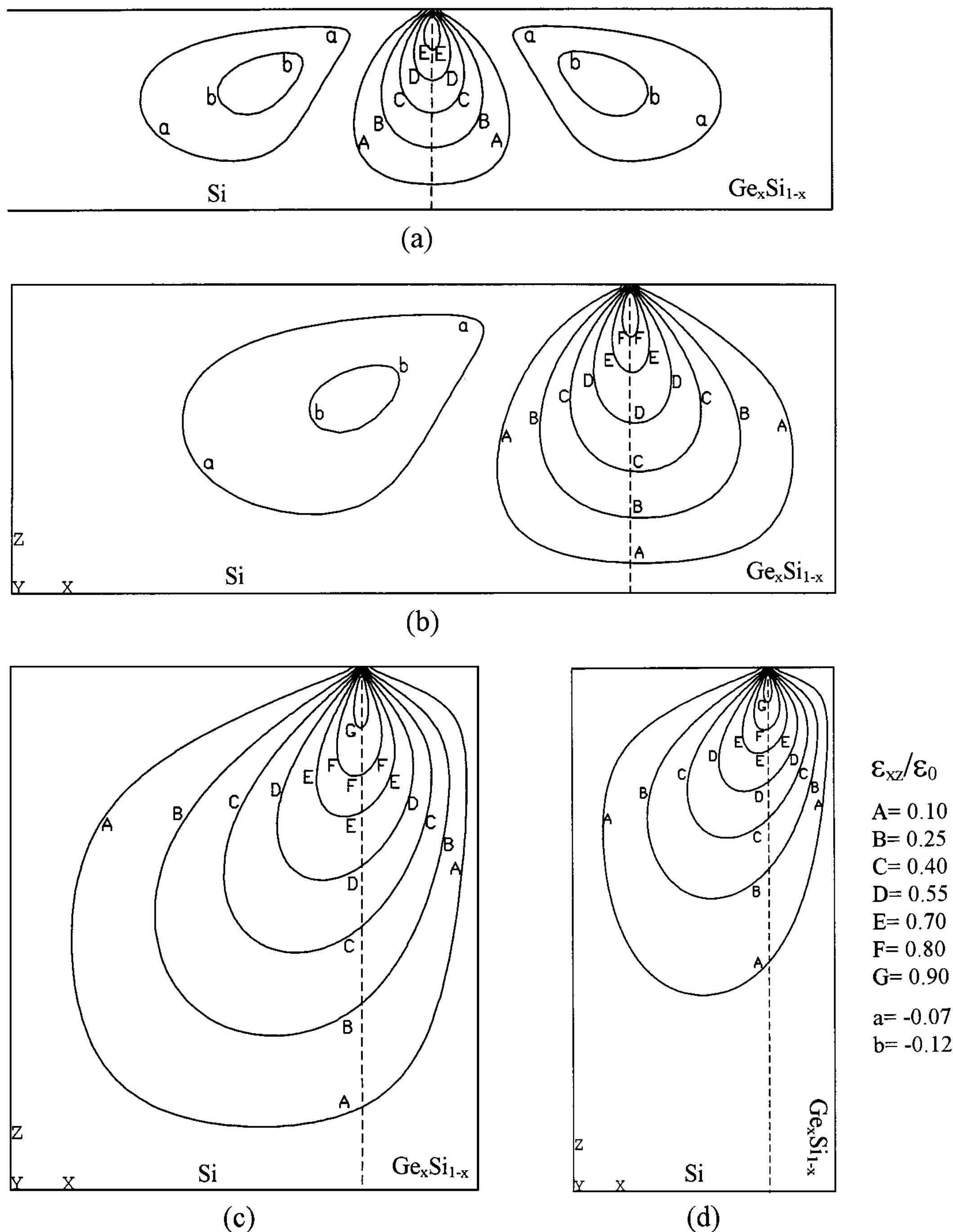

Figure 3 Distribution of the residual shear strain ε_{xz} in specimens: (a) $t/t_B = 1/2$; (b) $t/t_B = 3/2$; (c) $t/t_B = 9/2$; (d) $t/t_B = 8$. ($\varepsilon_0 = 0.3\%$ is the absolute value of residual strain ε_{zz} of material B in the bulk multilayer material.)

away from the interface, ε_{xx} becomes constant. When the specimen thickness is increased (Fig. 5b), the effect of surface on ε_{xx} in material B (Ge_xSi_{1-x}) is more obvious, i.e., at the region far from the interface the ε_{xx} becomes smaller with the distance away from the surface. When $t/t_A = 3/2$ and $t/t_B = 9/2$ (Fig. 5c), the ε_{xx} in material B (Ge_xSi_{1-x}) changes drastically near the surface. When both t/t_A and t/t_B are large (Fig. 5d), near the surface, ε_{xx} decreases drastically with the distance away from the surface; ε_{xx} becomes constant at the region far away from the surface. From Fig. 5c and d we know when the specimen thickness is larger than the material layer thickness, the maximal ε_{xx} of this layer locates at the intersection of the surface and the central axis of this layer.

3.4. Characteristics of the whole thickness average residual strains in specimens

When using CBED to study residual strains in the specimen, the measured residual strain values in the specimen are the average values of the whole thickness. Thus for making the numerical results useful to the CBED study, the FE results of residual strains in the specimen should be averaged throughout the thickness. The variations of the average strains $\overline{\varepsilon_{xz}}$, $\overline{\varepsilon_{zz}}$ and $\overline{\varepsilon_{xx}}$ along the x-axis are shown in Fig. 6, here $\overline{\varepsilon_{xz}}$, $\overline{\varepsilon_{zz}}$ and $\overline{\varepsilon_{xx}}$ are the whole thickness average strains. At the position $x = x_i$, the $\overline{\varepsilon_{xz}}$ is calculated by $\overline{\varepsilon_{xz}}(x_i) = (\Sigma_{j=1}^{N}(\varepsilon_{xz})_j V_j / V$, where N is the number of elements connected with the line $x = x_i$, $(\varepsilon_{xz})_j$ and V_j are the strain ε_{xz} and volume of the jth element connected with the line $x = x_i$, V

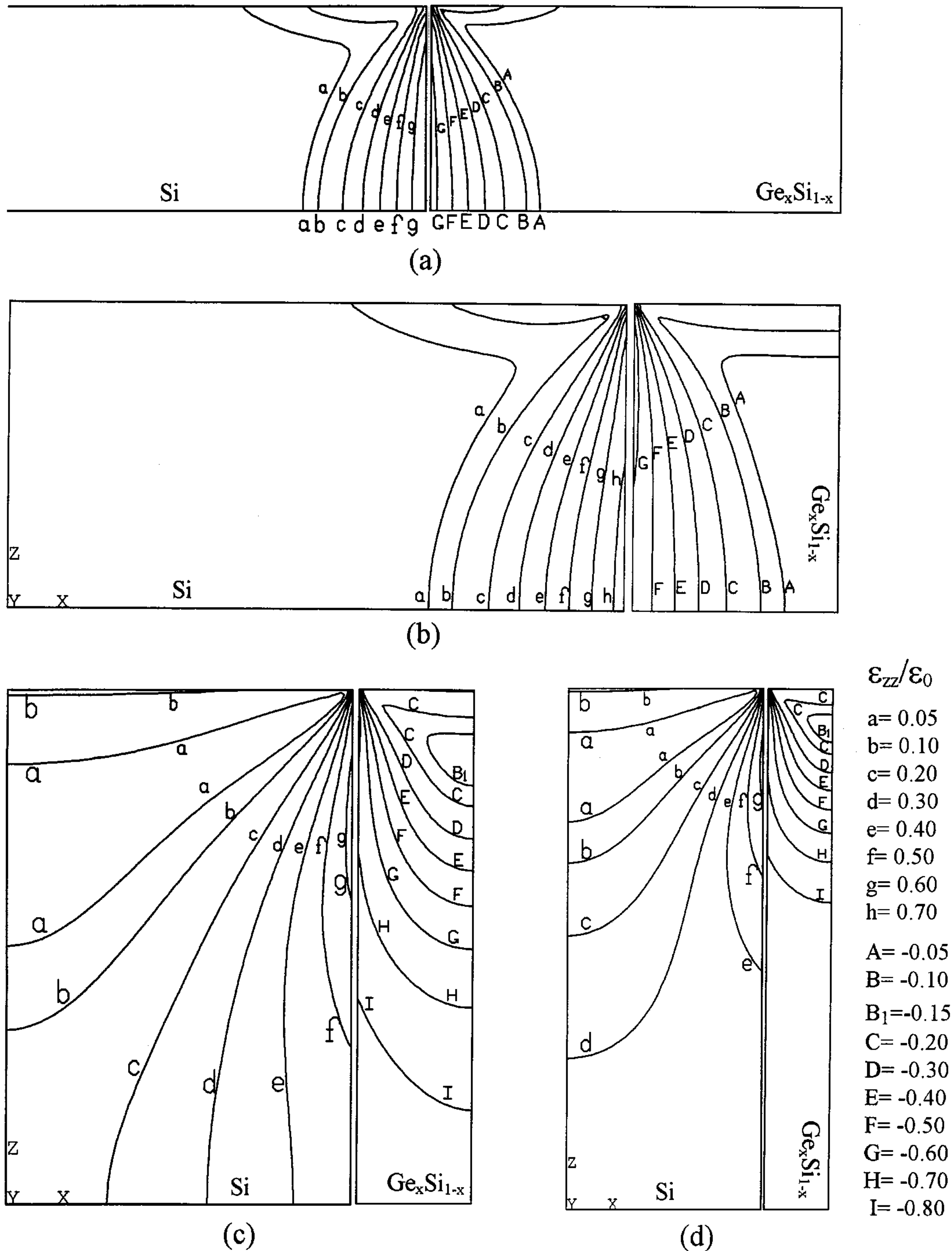

Figure 4 Distribution of the residual strain ε_{zz} in specimens: (a) $t/t_B = 1/2$; (b) $t/t_B = 3/2$; (c) $t/t_B = 9/2$; (d) $t/t_B = 8$. ($\varepsilon_0 = 0.3\%$ is the absolute value of residual strain ε_{zz} of material B in the bulk multilayer material.)

is the volume of all elements connected with the line $x = x_i$. At the position $x = x_i$, $\overline{\varepsilon_{zz}}$ and $\overline{\varepsilon_{xx}}$ are calculated in the similar way to $\overline{\varepsilon_{xz}}$. From Fig. 6 we can know how specimen thickness affects $\overline{\varepsilon_{xz}}$, $\overline{\varepsilon_{zz}}$ and $\overline{\varepsilon_{xx}}$, and how $\overline{\varepsilon_{xz}}$, $\overline{\varepsilon_{zz}}$ and $\overline{\varepsilon_{xx}}$ vary with the distance away from the interface.

When both t/t_A and t/t_B are small (Fig. 6a) ($t/t_A = 1/6$, $t/t_B = 1/2$), the largest $\overline{\varepsilon_{xz}}$, $\overline{\varepsilon_{zz}}$ and $\overline{\varepsilon_{xx}}$ locate at the interface; near the interface, $\overline{\varepsilon_{xz}}$, $\overline{\varepsilon_{zz}}$ and $\overline{\varepsilon_{xx}}$ become smaller drastically with the distance away from the interface; $\overline{\varepsilon_{xz}}$, $\overline{\varepsilon_{zz}}$ and $\overline{\varepsilon_{xx}}$ become constant at the region far from the interface; near the interface, $\overline{\varepsilon_{xz}}$ is symmetrical about the interface, and the absolute value of $\overline{\varepsilon_{zz}}$ is nearly symmetrical about the interface. With the increase of specimen thickness (Fig. 6b) ($t/t_A = 1/2$, $t/t_B = 3/2$), the region affected by $\overline{\varepsilon_{xz}}$ becomes wider; the symmetry of $\overline{\varepsilon_{xz}}$ about the interface is lost. From Fig. 6c ($t/t_A = 3/2$, $t/t_B = 9/2$) and Fig. 6d ($t/t_A = 4/3$, $t/t_B = 4$), we see that for thick specimen, the relationship between $\overline{\varepsilon_{xz}}$ and the distance away from the interface becomes linearly; with the increase of specimen thickness, the distributions of $\overline{\varepsilon_{zz}}$ and $\overline{\varepsilon_{xx}}$ become smoother.

3.5. Availability of the method described above

The method described above can be conveniently applied to model the stress relaxation of thin specimens. The basic idea is: put the FE model of the specimen into

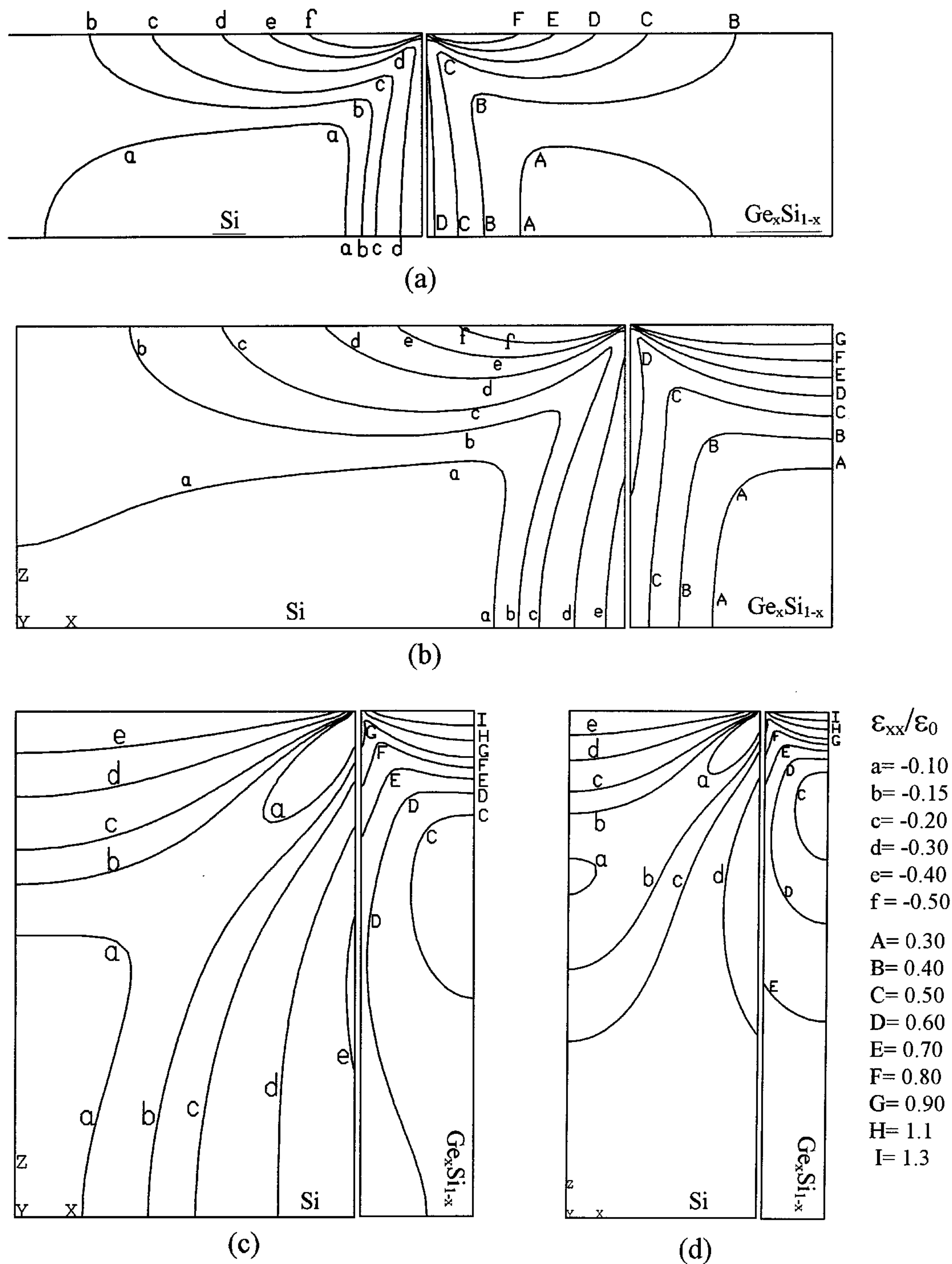

Figure 5 Distribution of the residual strain ε_{xx} in specimens: (a) $t/t_B = 1/2$; (b) $t/t_B = 3/2$; (c) $t/t_B = 9/2$; (d) $t/t_B = 8$. ($\varepsilon_0 = 0.3\%$ is the absolute value of residual strain ε_{zz} of material B in the bulk multilayer material.)

the FE model of the bulk material, and determine the initial residual stresses and strains in the bulk material; then separating the FE model of the specimen from the FE model of the bulk material by deactivating the elements outside the FE model of the specimen. In real cases, it is often that the residual strains in the thin specimen are known, while the residual strains in the bulk material are unknown. We can assume a set of values to the residual strains or stresses in the bulk material, then model the residual strains in the specimen after stress relaxation; compare the FE results with the measured results, then adjust the assumed residual strains values in the bulk material, and model the elastic relaxation again. In this way, residual strains in the bulk material can be deduced. This method can be applied to model elastic relaxation in CBED specimens of many materials, such as metal matrix composites [1, 2], Strained-layer superlattices [3–5], Nickel based superalloys [6], deformed copper [7, 8], epitaxical systems [9, 10], etc.

4. Conclusions

A procedure for modeling effects of surface stress relaxation during processing specimens from the bulk material with residual stresses has been described in this paper. Based on the FE results, characteristics of residual strains in the cross-sectional specimen of strained-layer material are concluded as follows:

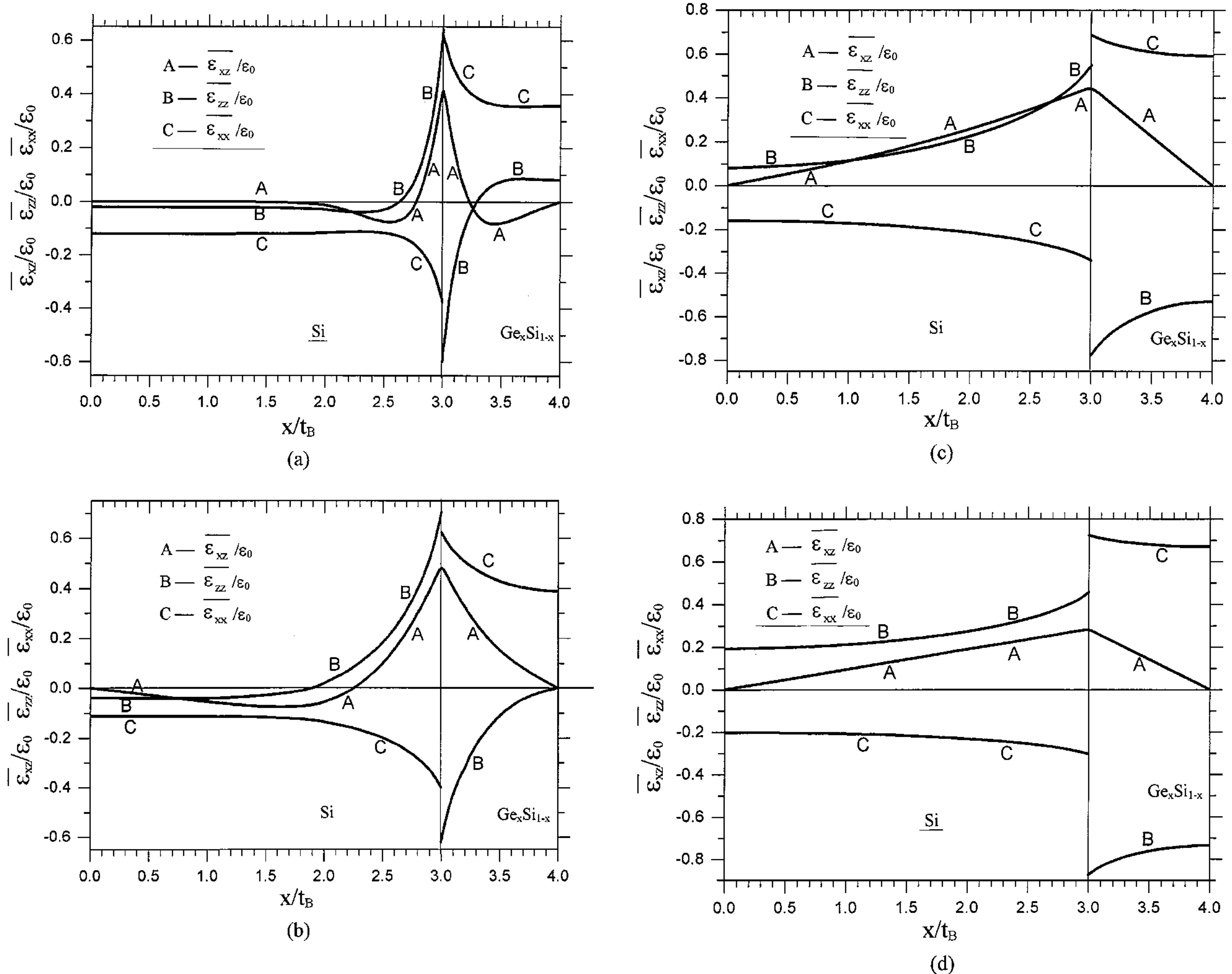

Figure 6 Distributions of the average residual strains $\overline{\varepsilon_{xz}}$, $\overline{\varepsilon_{zz}}$ and $\overline{\varepsilon_{xx}}$ in specimens ($\overline{\varepsilon_{xz}}$, $\overline{\varepsilon_{zz}}$ and $\overline{\varepsilon_{xx}}$ are the average strains of the whole thickness of specimen): (a) $t/t_B = 1/2$; (b) $t/t_B = 3/2$; (c) $t/t_B = 9/2$; (d) $t/t_B = 8$. ($\varepsilon_0 = 0.3\%$ is the absolute value of residual strain ε_{zz} of material B in the bulk multilayer material.)

Within the strained-layer material, there is no residual shear strain ε_{xz}. In the cross-sectional specimen of such material, residual shear strain ε_{xz} is created at the interface near the surface. The maximal ε_{xz} locates at the local interface region a little below the surface. The maximal ε_{xz} is affected by the ratio of specimen thickness to material layer thickness. The smaller this ratio is, the smaller the maximal ε_{xz} will be. This shear strain is zero at the center of each material layer, and is also zero at the thickness center of specimen.

Residual strain ε_{zz} is larger at the interface, and decreases with the distance away from the interface. The smallest ε_{zz} is not at the surface, but a little distance away from the surface.

Residual strain ε_{xx} is larger at the surface than at the inside of specimen. When the specimen thickness is larger than the material layer thickness, the maximal ε_{xx} of this layer locates at the intersection of the surface and the central axis of this layer.

The local region at the intersection of interface and surface is a special region, where residual strains ε_{xz}, ε_{zz} and ε_{xx} change drastically with the distance away from the interface or surface.

The whole thickness average residual strains $\overline{\varepsilon_{xz}}$, $\overline{\varepsilon_{zz}}$ and $\overline{\varepsilon_{xx}}$ are largest at the interface, and decrease with the distance away from the interface.

Acknowledgements
The work was financially supported by the National PAN-Deng project (Grant No. 95-YU-41) of China.

References
1. S. J. ROZEVELD, J. M. HOWE and S. SCHMAUDER, *Acta Metall. Mater.* **40** (1992) S173.
2. H. M. ZOU, J. LIU, D. H. DING, R. H. WANG, L. FROYEN and L. DELACY, *Ultramicroscopy* **72** (1998) 1.
3. D. D. PEROVIC, G. C. WEATHERLY and D. C. HOUGHTON, *Phil. Mag. A*, **64** (1991) 1.
4. X. F. DUAN, D. CHERNS and J. W. STEEDS, *ibid.* **70** (1994) 1091.
5. A. ARMIGLIATO, R. BALBONI, F. CORTICELLI, S. FRABBONI, F. MALVEZZI and J. VANHELLEMONT, *Mater. Sci. Techn.*, **11** (199) 400.
6. R. VÖLKL, U. GLATZEL and M. FELLER-KNIEPMEIER, *Acta Mater.*, **46** (1998) 4395.
7. H. J. MAIER, H. RENNER and H. MUGHRABI, *Ultramicroscopy*, **51**, (1993) 136.
8. R. R. KELLER, H. J. MAIER, H. RENNER and H. MUGHRABI, *Phil. Mag. A*, **70**, (1994) 329.
9. F. BANHART and N. NAGEL, *ibid.* **70** (1994) 341.
10. R. BALBON, S. FRABBONI and A. ARMIGLIATOR, *ibid.* **77** (1998) 67.
11. H. J. MAIER, R. R. KELLER, H. RENNER, H. MUGHRABI and A. PRESTON, *ibid.* **74**, (1996) 23.
12. J. M. GIBSON and M. M. J. TREACY, *Ultramicroscopy*, **14** (1984) 345.

13. M. M. J. TREACY, J. M. GIBSON and A. HOWIE, *Phil. Mag. A.*, **51** (1985) 389.
14. M. M. J. TREACY and J. M. GIBSON, *J. Vac. Sci. Technol.* **B4**, (1986) 1458.
15. D. JACOB, Y. ANDROUSSI, T. BENABBAS, P. FRANCOIS and A. LEFEBVRE, *Phil. Mag. A.*, **78** (1998) 879.
16. K. N. TU, J. W. MAYER and L. C. FELDMAN, in "Electronic Thin Film Sciences: For Electrical Engineers and Material Scientists," (Macmillan College Publishing Company, Inc. 1992) appendix E.
17. C. R. CHEN, S. X. LI and Z. G. WANG, *Mater. Sci. Eng. A*, **247** (1998) 15.

Received 10 March
and accepted 25 August 1999